ACS OMEGA

Open Access

http://pubs.acs.org/journal/acsodf

Article

Highly Durable Antibacterial Textiles: Cross-Linked Protonated Polyaniline-Polyacrylic Acid with Prolonged Electrical Stability

Muhammad Faiz Aizamddin,* Zaidah Zainal Ariffin, Nur Asyura Nor Amdan, Mohd Azizi Nawawi, Nur Aimi Jani, Muhd Fauzi Safian, Siti Nur Amira Shaffee, Nik Mohd Radi Nik Mohamed Daud, Maung Maung Myo Thant,* and Mohd Muzamir Mahat*

Cite This: *ACS Omega* 2024, 9, 23303−23315

Read Online

ACCESS | Metrics & More | Article Recommendations | Supporting Information

ABSTRACT: This study addressed the limited antibacterial durability of textile materials, which has suppressed their applications in preventing infectious disease transmission. A class of highly durable antibacterial textiles was developed by incorporating protonated polyaniline (PANI) textile with poly(acrylic acid) (PAA) as the functional binder via cross-linking polymerization. The resulting PAA−PANI textile exhibits exceptional electrical conductivity, reaching 8.33 ± 0.04 × 10^{-3} S/cm when cross-linked with 30% PAA. Remarkably, this textile maintains its electrical stability at 10^{-3} S/cm even after 50 washing cycles, demonstrating unparalleled durability. Furthermore, the PANI−PAA textile showcases remarkable antibacterial efficacy, with 95.48% efficiency against *Pseudomonas aeruginosa* and 92.35% efficiency against *Staphylococcus aureus* bacteria, even after 50 washing cycles. Comparatively, the PAA−PANI textile outperforms its PANI counterpart by achieving an astounding 80% scavenging activity rate, whereas the latter only displayed a rate of 3.22%. This result suggests a solid integration of PAA−PANI into the textile, leading to sustainable antioxidant release. The successful cross-linking of PAA−PANI in textiles holds significant implications for various industries, offering a foundation for the development of wearable textiles with unprecedented antibacterial durability and electrical stability. This breakthrough opens new avenues for combating infectious diseases and enhancing the performance of wearable technologies.

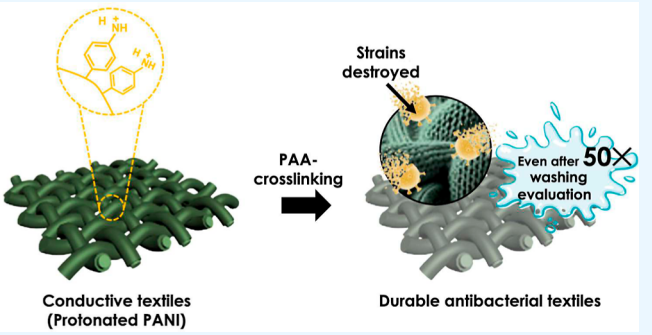

1. INTRODUCTION

Over the past few years, wearable textiles have experienced significant growth in interest, mainly due to their promising capabilities in offering continuous monitoring and treatment options for various medical conditions.[1,2] The flexibility and comfort of these textiles are two of their prime characteristics. For instance, wearable textiles can monitor vital signs such as heart rate, blood pressure, and oxygen saturation. This proactive monitoring enables early detection of health issues and a timely intervention. Nevertheless, the looming perils of infectious diseases have accentuated the beneficial influence of antibacterial textiles in mitigating the proliferation of such outbreaks.[3] However, the proliferation of bacterial contaminants may potentially undermine wearable textiles' efficacy. This risk has become a driving force behind rendering antibacterial properties to wearable textiles. Optimizing antibacterial properties and conductivity in wearable textiles requires a thorough understanding of the textile's field performance. Historically, the integration of functional metals such as silver (Ag), reduced graphene oxide, titanium dioxide (TiO_2), and copper oxide (Cu_2O) with textiles has been extensively employed to instill remarkable electrical conductivity and robust antibacterial characteristics.[4,5] Nevertheless, the integration of such metal-based materials might adversely affect the environment with the outcome of diminishing textile comfort.[6,7]

As a conducting polymer, polyaniline (PANI) offers an alternative due to its low toxicity, tunable electrical properties, biocompatibility, and ease of preparation.[8,9] In a recent review, protonated PANI textiles showed outstanding electrical conductivity and strong antibacterial properties against Gram-positive and Gram-negative bacteria.[10] Dhivya et al. discovered that protonated PANI exhibited a remarkable 2-fold increase in antibacterial efficacy compared to that of its deprotonated counterpart when tested against an array of Gram-positive bacterial species and fungi.[11] Omar et al. showed that PANI, with an optimal concentration of 30%

Received: December 10, 2023
Revised: February 24, 2024
Accepted: February 29, 2024
Published: May 23, 2024

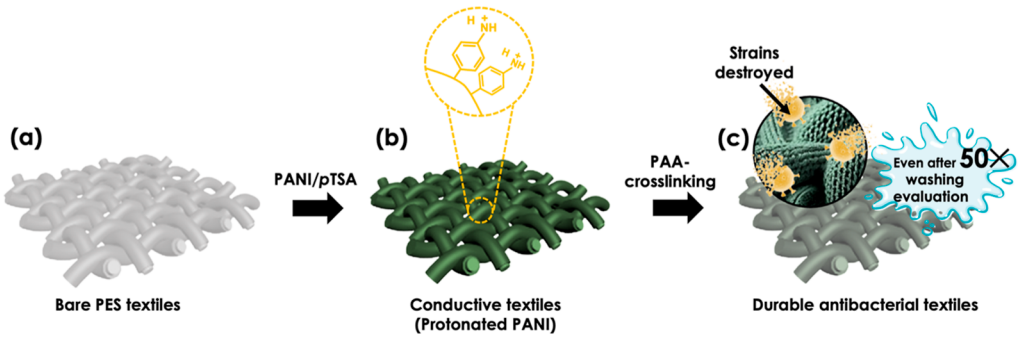

Figure 1. Schematic of the fabrication of the durable antibacterial PAA−PANI textile. (a) Pristine polyester (PES) textile. (b) Pristine PES textile integrated with conductive and antibacterial agents from PANI solution. (c) PAA as the secondary polymer binder is introduced onto the functional textile by cross-linking polymerization aiming to improve its antibacterial durability.

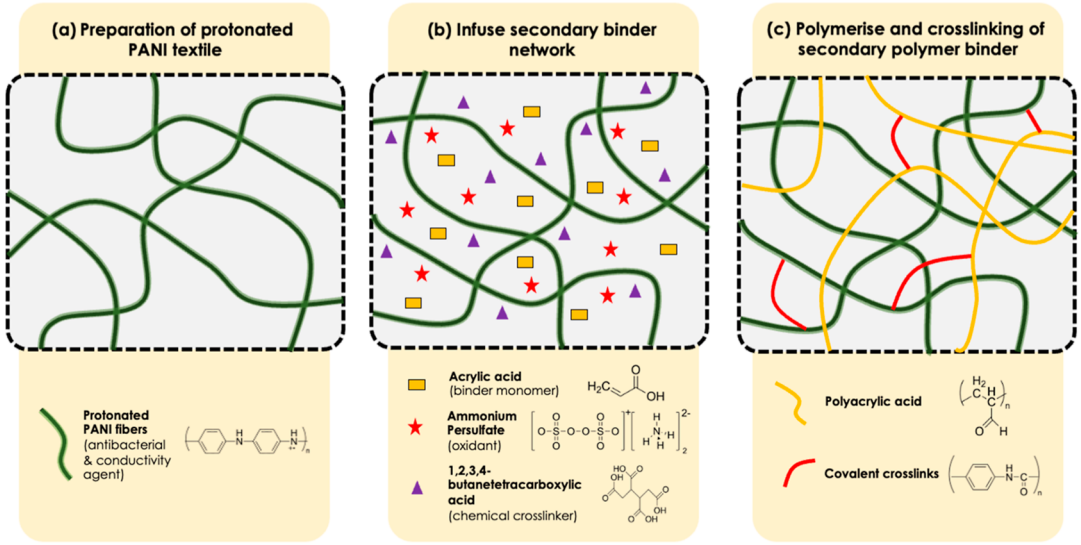

Figure 2. Illustration of chemical structure formation of the PAA−PANI textile at different conditions. (a) The PANI textile was prepared through immersion of conductive PANI solutions onto the textile. (b) The PANI textile was immersed in a PAA precursor solution of AA, APS, and BATC. Each constituent functioned as a secondary binder network, oxidant, and chemical cross-linker, respectively. (c) Finally, the polymerization and cross-linking of the PAA−PANI textile were accomplished at a temperature of 70 °C.

(v/v) phytic acid, had an impressive electrical conductivity of 2.15 × 10^{-2} S/m. This effective combination displayed excellent antibacterial qualities, successfully fighting off strains of *Klebsiella pneumoniae*, *Staphylococcus aureus*, and *Escherichia coli*.[12] When protonated PANI polycations attach to negatively charged bacterial surfaces, they create an extra barrier that disrupts the bacterial activities. As Maruthapandi et al. mentioned, the molecular weight of the protonated polymer plays a crucial role in its permeability through the bacterial cell wall.[13] Nonetheless, the employment of protonated PANI for its antibacterial properties remains constrained due to its limited infusibility and solubility.[14] The antibacterial attributes of PANI may progressively wane as time elapses, potentially resulting in an accumulation of bacteria and various microorganisms upon the textile's surface. The manifestation can infect surfaces, possibly increasing the risk of infection. To address these issues, researchers are exploring alternative methods to maintain antibacterial properties in textiles including antibacterial agents. For example, Erdem and Rajendran treated knitted and nonwoven fabrics with antibacterial silver ions via the pad-cure technique.[15] Dariush et al. designed a cotton/polyester fabric for drug-loaded nanofibers via electrospinning and investigated the nanofibers' performance.[16] Nabipour's recent study utilized cotton fabric treated with Ag and Zn ion-rich guanazole complexes. The treated cotton displayed a broad spectrum of antimicrobial activity against bacterial and fungal pathogens.[17] These ground-breaking advancements catalyze the evolution of antimicrobial textiles.

In addition to adhering to a stringent efficacy, optimized antimicrobial fabrics must satisfy the rigorous benchmarks of resilience and environmental sustainability. Incorporated textiles are an excellent choice for loading antibacterial agents because they offer higher loading capabilities, greater flexibility of polymers and drugs, and better encapsulation efficiency. Despite their potential, the obstacle of retaining the antibacterial loading into substrate materials remains a point of contention.[18] Various techniques to augment the antibacterial agent's adhesion onto textiles and retain its antibacterial properties have been explored, such as treating cotton fabric with an alkali solution, plasma electrospinning to form active chemical surface groups, and mixing the electrospun solution with high-temperature adhesive powder.[19−22] Nevertheless, the antibacterial longevity of such coatings is significantly compromised after approximately five laundering cycles due to their tenuous adherence to the textile.[23,24]

https://doi.org/10.1021/acsomega.3c09871
ACS Omega 2024, 9, 23303−23315

This research presents the development of antibacterial textiles by incorporating protonated PANI as a conductive and antibacterial agent onto the polyester textile. The cross-linking polymerization of poly(acrylic acid) (PAA) was employed as a functional binder to the textile, forming intermolecular bonds between polymer chains. This pioneering technology enables the creation of textiles with long-lasting antibacterial activity and remarkable electrical capabilities without sacrificing their resilience. The fabrication of the durable antibacterial PANI−PAA textile is illustrated in Figure 1.

2. MATERIALS AND METHODS

2.1. Materials. Pristine (PES textile (50 cm × 50 cm) was purchased from Kamdar Sdn. Bhd. (Klang, Malaysia). Polyaniline emeraldine base (PANI-EB) solution, *para*-toluene sulfonic acid (*p*TSA), and acrylic acid (AA) were sourced from Sigma-Aldrich (St. Louis, MO, USA). 1,2,3,4-Butanetetracarboxylic acid (BATC) and ammonium persulfate $(NH_4)_2S_2O_8$ were purchased from Merck (Darmstadt, Germany).

2.2. Preparation of the Protonated PANI−PAA Textile. The preparation and chemical structure formation of the PAA−PANI textile are illustrated in Figure 2. A knitted PES textile was trimmed to a designated dimension of 5 cm × 5 cm and immersed in a protonated PANI solution. The solution was prepared by doping PANI with *p*TSA at an optimized value of 6.21×10^{-3} S/cm. This optimization was recorded from the analysis, as detailed in Figure S1. The textile was submerged in the protonated PANI solution for 30 min, followed by drying at room temperature in total darkness (Figure 2a). Subsequently, the PANI textile was soaked in the PAA precursor solution (PAAc). The PAAc was a mixture of 10 v/v % AA, APS as initiator, and BATC as cross-linker in a 2:1:1 volume ratio (Figure 2b). The polymerization of PAA through chemical oxidation was conducted by stirring the mixture for 4 h. Afterward, the PANI−PAA textile was taken out from the solution and placed in an oven operated at 70 °C for 30 min to activate the PAA cross-linking (Figure 2c). Finally, the textile was rinsed with distilled water to remove the PAA residue. The procedure was repeated with other concentrations of AA in PAAc, i.e., 20, 30, 40, and 50 v/v %.

2.3. Characterizations of the PAA−PANI Textile. The functional group of the fabricated textile was identified with attenuated total reflectance−Fourier transform infrared (ATR−FTIR) analysis (version 10, PerkinElmer, Ltd., London, UK). Electrochemical impedance spectroscopy (EIS) (model: HIOKI 3532-50 LCR-HI Tester, HIOKI E. E. Corporation, Nagano, Japan) measured the electrical conductivity of the textile samples. The analysis was performed at room temperature within a frequency range of 100 Hz−1000 kHz. The 5 × 5 cm textile was clamped between two copper electrodes with a diameter of 1 cm. The thickness of the textile was measured beforehand with a digital thickness gauge. An average of three measurements was recorded. The conductivity of the textile was derived from the following expression 1[25−27]

$$\sigma = L/(R_b \times A) \quad (1)$$

where L is the thickness of the textile, R_b is the bulk resistance of the fabric from the Nyquist data, and A is the area of the electrodes. The surface morphology of the PAA−PANI textile was observed with a SNE-4500 M Plus Tabletop scanning electron microscope that was equipped with energy-dispersive X-ray to ascertain the elemental compositions of samples. The textile was sputtered with a ∼10 nanometer gold film to improve the image's resolution. The textile was cut in 1 cm × 1 cm before the images were captured within a magnification range of 600−12,000×. The textile's mechanical strength was analyzed with a universal strength tester machine (model: Tenso Lab 5000, MESDAN S.P.A., Puegnago del Garda (BS)-Italy). The mechanical testing complied with the ASTM D5035-95 protocol. The textiles in 4 cm × 7.5 cm dimensions were prepared and tested under the condition of a constant crosshead speed of 300 mm/min transverse rate and 5 kN load force. Tensile stress and percentage elongation at break were recorded from the analysis as displayed in Figure S2a,b. The water contact angle of the textile was evaluated with a Theta Lite Optical Tensiometer (Contact Angle Meter, Phoenix, United States). During the measurement, 3 μL droplets of distilled water were carefully positioned on the textile using a microliter syringe. Each contact angle value was equivalent to the average of at least five contact angle measurements at various spots on the textile.

2.4. Washing Durability Evaluation. The simplified version of standard test methods 132-2004 and 86-2005 from the American Association of Textile Chemists and Colorist were adopted to evaluate textile durability.[28] The nontreated and treated PANI textiles were sewn at all edges to ensure consistent results over the entire surface. The textiles were then submerged in a 200 mL TTE detergent solution and agitated at 60 °C for 30 min in metal-capped bottles. After each treatment, the textiles were dried for an hour in a ventilated hood at 27 °C before characterization. This process was repeated for 50 cycles for electrical measurements and 15 cycles to evaluate the antibacterial activities. Diagrams of PANI textile washing evaluation, electrical measurement, and antibacterial testing can be found in Figure S2c.

2.5. Kirby−Bauer Disk Diffusion. Two isolates of bacteria; *Staphylococcus aureus* (ATCC25923) and *Pseudomonas aeruginosa* (ATCC27853) were employed to test the antibacterial performance of the PANI−PAA textile. The bacteria isolates (4.0×10^{-5} CFU/mL) were inoculated in Mueller Hinton (MH) broth and incubated at 37 °C for 24 h under 250 rpm shaking conditions. The bacterial suspension's turbidity was adjusted to fulfill the 0.5 McFarland standard by adding phosphate-buffered saline (PBS) (1×). Using a sterile cotton swab, the MH agar was lawned with each bacterial isolate. The specimens (6.05 ± 0.08 mm^2) were placed on the agar with sterilized tweezers, including the control antibiotic discs for each strain (positive control), pristine PES textile (negative control), and PANI−PAA textile. The plates with lawned bacteria and specimens were incubated at 37 °C for 18 h. The appearance and size of the inhibition zone around the specimens were measured, as illustrated in Figure S3. Measurements were performed in triplicate. Based on the resulting inhibition zone, the antibacterial effectiveness rate of the PAA−PANI textile against both bacteria was calculated with formula 2

$$\text{Antibacterial rate of efficiency} = ((A - B)/A) \times 100\% \quad (2)$$

where A is the inhibition zone diameter without washing and B is the inhibition zone diameter after washing. This formula determines the percentage decrease in the inhibition zone diameter following a wash. The percentage was subtracted from 100% to derive the postwash bacterial growth inhibition percentage. The calculation was repeated for 50 washing cycles.

https://doi.org/10.1021/acsomega.3c09871
ACS Omega 2024, 9, 23303−23315

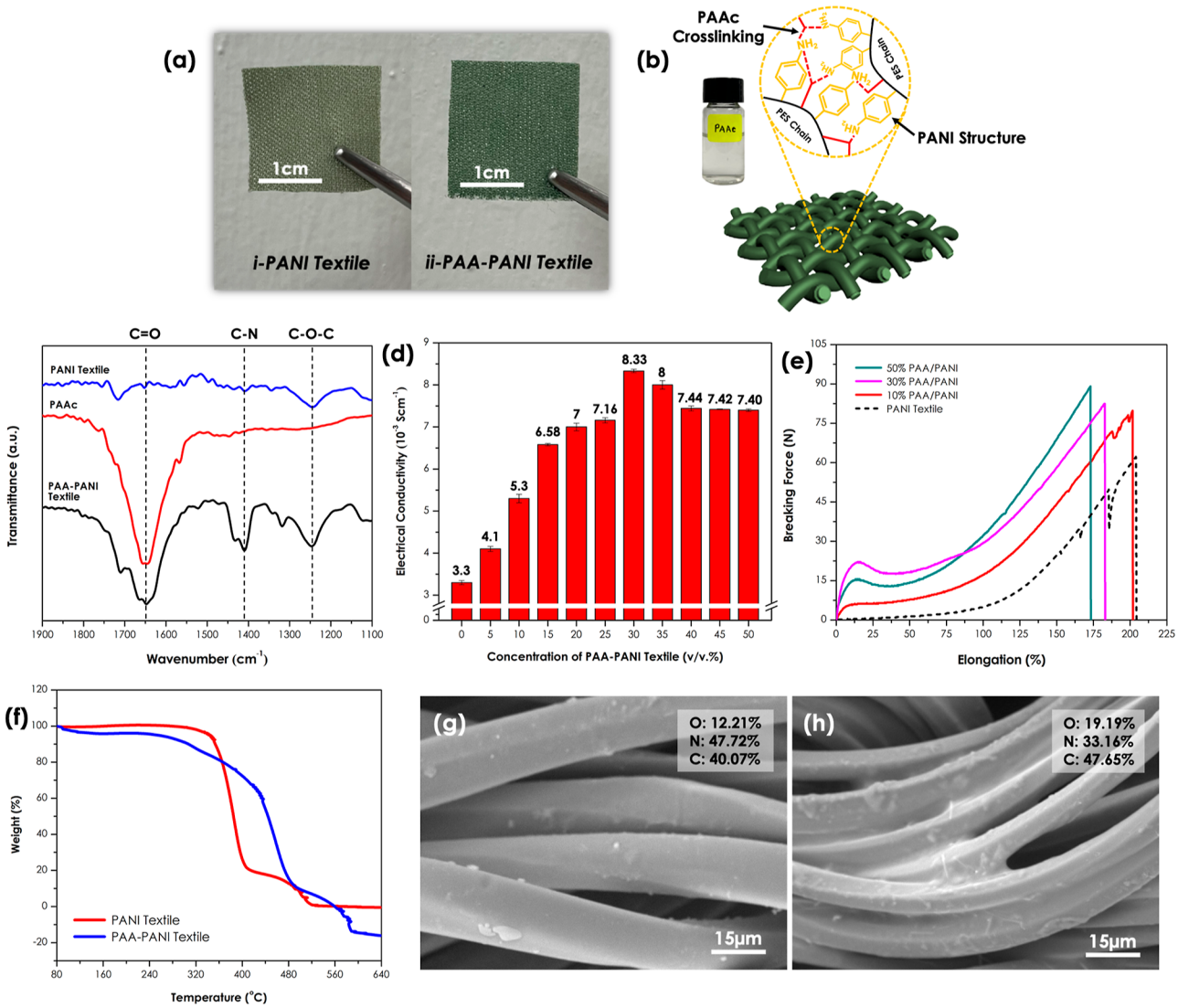

Figure 3. (a) Physical appearances of (i) PANI and (ii) PAA−PANI textiles. (b) Chemical interactions between PAAc and PANI textiles. (c) IR spectra of PANI, PAAc, and PAA−PANI textiles. (d) Comparison of PANI textiles' electrical conductivity with different binders. (e) Breaking force−elongation curve of different amounts of PAA in PANI textiles. (f) TGA thermograms for pristine PES, PANI, and PAA−PANI textiles. 600× magnification surface morphology of (g) PANI fibers and (h) PAA−PANI fibers with elemental compositions.

2.6. DPPH Radical-Scavenging Assay. 1,1-Diphenyl-2-picrylhydrazyl (DPPH) radical-scavenging activity was performed to determine the antioxidant activity of each textile. In the test tube, 10 mg of textile was immersed in a 1.6 mL of 0.1 mM DPPH-methanol solution. The spectra of the solutions were recorded at 517 nm spectrum using an ultraviolet spectrophotometer (model: Secomam Prim Light, Aqualabo Group, Shanghai, China). In this method, the absorbance spectrum of control sample (i.e., free radical-scavenging activity) was compared to that of the sample that was exposed to radical-scavenging activity following a 30 min incubation period at 25 °C in total darkness. A lower absorbance indicated higher DPPH radical-scavenging activity in the reaction mixture. The test was repeated three times. The textile's scavenging activity percentage (%) was derived from formula 3

$$\text{DPPH scavenging activity}(\%) = ((B - A)/A) \times 100 \quad (3)$$

where A and B represent the absorbance of the sample from the textile and the untreated textile, respectively.

3. RESULTS AND DISCUSSION

3.1. Physical and Chemical Characterizations of the PAA−PANI Textile. Antibacterial textiles must meet the criteria of exhibiting exceptional conductivity and antibacterial properties. Unfortunately, washing cycles can compromise the coating's durability due to the topical coverage of antibacterial agents on the textile. The leaching of the dopant anion after washing can harm the electrical insulation of the textile. Introducing a unique functional binder in this study offered dual advantages. First, the binder supported the creation of an effective electron transport pathway. Second, the sustainability of antibacterial loading was reinforced due to the substantial interaction between the binder and the functional groups of the textile.

In Figure 3a(i), the green color of the protonated PANI textile signaled its conductive emeraldine salt state before PAA cross-linking.[29] After PAAc was introduced, the PANI textile changed to a darker green due to its degree of oxidation, as seen in Figure 3a(ii). According to Namsheer, as the polymer oxidizes, the length of the conjugated π-system increases and

https://doi.org/10.1021/acsomega.3c09871
ACS Omega 2024, 9, 23303−23315

augments light absorption.[30] This theory justifies the lighter green in the less oxidized PANI.

Hydrophilic PAAc is infused easily into the PANI textile. Subsequently, the heat was introduced to initiate the structural cross-linking. During this process, cation radicals ($-NH_3^+$) from the PANI chains combined with the PAA network of anion radicals (−COO−) via strong electrostatic interactions and intermolecular hydrogen bonds (Figure 3b). This combination led to an interpenetrating polymer network with an improved mechanical strength.

The postadsorption IR spectra of PANI, PAA, and PANI−PAA textiles are presented in Figure 3c. The firm absorption peaks at 1649.56 cm^{-1} were attributed to the carboxylic group's C═O from PAAc and PANI−PAA textiles. In the PAA−PANI spectrum, the characteristic absorption bands at 1410.26 cm^{-1} were attributed to the C−N of a secondary aromatic amine and the C−N stretching vibration in a B−NH−B−NH unit (B is a benzenoid ring). Additionally, new noteworthy bands at 1343.20 and 1378.16 cm^{-1} appeared in the spectrum of PAA−PANI, indicating a robust hydrogen bonding between PAA and PANI textiles. The peak at 1246.82 cm^{-1} alluded to carboxylate's asymmetric C−O−C, which could be assigned to the O−C in-plane bending and C−O out-of-plane bending vibrations, respectively. These observations illuminated the presence of steadfast intermolecular hydrogen bonds intertwining the PAA and PANI chains, laying the foundation for interpenetrating polymer networks. Furthermore, these spectral characteristics indicated some degree of cross-linking between their chains.

The electrical conductivity of the PAA−PANI textile in different concentrations of PAA is illustrated in Figure 3d. This characterization aimed to identify the optimum concentration of PAA. The data is presented in Table 1. Protonated PANI

Table 1. Electrical Conductivity of PAA−PANI Textiles in Different Concentrations of PAA

concentration of PAA−PANI (v/v %)	electrical conductivity ($\times 10^{-3}$ S/cm)
0	3.30 ± 0.05
5	4.10 ± 0.06
10	5.30 ± 0.10
15	6.58 ± 0.03
20	7.00 ± 0.09
25	7.16 ± 0.06
30	8.33 ± 0.04
35	8.00 ± 0.10
40	7.44 ± 0.06
45	7.42 ± 0.01
50	7.00 ± 0.03

textile had a conductivity of 3.3 ± 0.45 × 10^{-3} S/cm, which aligned with previous findings. The conductivity of the PAA−PANI textile jumped from 4.10 ± 0.06 to 8.33 ± 0.04 × 10^{-3} S/cm when the PAA content was increased from 5% to 30%. Overall, there was a dynamic relationship between PAA concentration in PANI textiles and conductivity. Incorporating PAA into PANI preceded a robust electrical network in the polymer. Due to the network, electrons could easily migrate along the polymer backbone to conduct electricity. The highest electrical conductivity was discovered with 30% PAA in PANI. However, increasing the concentration of PAA was counterproductive. The conductivity dropped from 8.00 ± 0.10 × 10^{-3} to 7.00 ± 0.03 × 10^{-3} S/cm when the PAA concentration in PANI was raised from 35 to 50%. Probably, as the concentration of PA in PANI was raised beyond 50%, the structure of the polymer become too dense and less flexible, which suppresses the electrical conductivity.

The PAA−PANI textile mechanical test outcomes are tabulated in Table 2, while Figure 3e shows the breaking

Table 2. Breaking Force and Elongation of the PAA−PANI Textile in Different Concentrations of PAA

textile	breaking force (N)	elongation (%)
PANI	62.26	204.00
10% PAA/PANI	78.57	201.58
30% PAA/PANI	81.83	182.33
50% PAA/PANI	88.56	172.38

force−elongation curves of all textiles. Both tensile stress and elongation are crucial mechanical properties for textiles, signifying their flexibility for wearable electronics applications. In this study, PANI textiles without PAA had the lowest breaking force of 62.26 N. The addition of a 10% PAA binder augmented physical interaction with the PANI textile. The intermolecular interactions between polymer chains were intensified as the breaking force curve reached 78.57 N. At this point, the textile became more robust and resilient.

Additionally, the $\pi-\pi$ interaction between the aromatic ring of PANI and PAA played a crucial role in the stress distribution. The trends increased as the concentration of PAA increased from 30 to 50%, with 81.83 and 88.56 N, respectively. Nevertheless, increasing PAA concentration reduced textile elongation, with a 1% drop in the elongation rate for every 10% PAA addition. In contrast, adding 30 and 50% PAA minimized the elongation rate of PANI textiles by 11 and 18.34%, respectively. Judging from the tensile and conductivity tests, the optimum concentration of PAA in PANI was 30% due to its moderate mechanical properties and the highest electrical conductivity value.

The thermogravimetric analysis (TGA) curves of PANI and PAA−PANI textiles displayed two degradation stages (Figure 3f). The major decomposition of PAA−PANI (77.34%) and PANI textiles (81.42%) was initiated at 257.36 and 338.32 °C, respectively. During this phase, the PANI functional groups began to decompose. Different degradation trends between the two samples indicate that PAA is successfully incorporated in the PANI structure. Although the PAA−PANI textile had an earlier degradation point, its degradation phase ended at 487.68 °C, which was higher than that of the PANI textile at 406.39 °C. This major shift in degradation point implied an improvement in the thermal stability of the PAA−PANI textile. This observation was derived from the decarboxylation of carboxylic acid on PAA segments, which required higher energy to break the carbon chains.[31] In the final stage, 22.66% of PAA−PANI and 18.58% of PANI fibers were fully decomposed at 590.46 and 519.29 °C, respectively. A slight reduction was distinguished due to the excess of polymer linkage along with the formation of PAA−PANI segments. This finding indicated improved thermal stability due to the cross-linking of PAA with the PANI textile.

Figure 3g,h shows the morphological images of PANI and PAA−PANI fibers with their respective elemental compositions. The cross-linking of PAA with PANI textile significantly changed the morphology of the fibers. PANI fibers typically display a homogeneous surface due to the regular arrangement

https://doi.org/10.1021/acsomega.3c09871
ACS Omega 2024, 9, 23303−23315

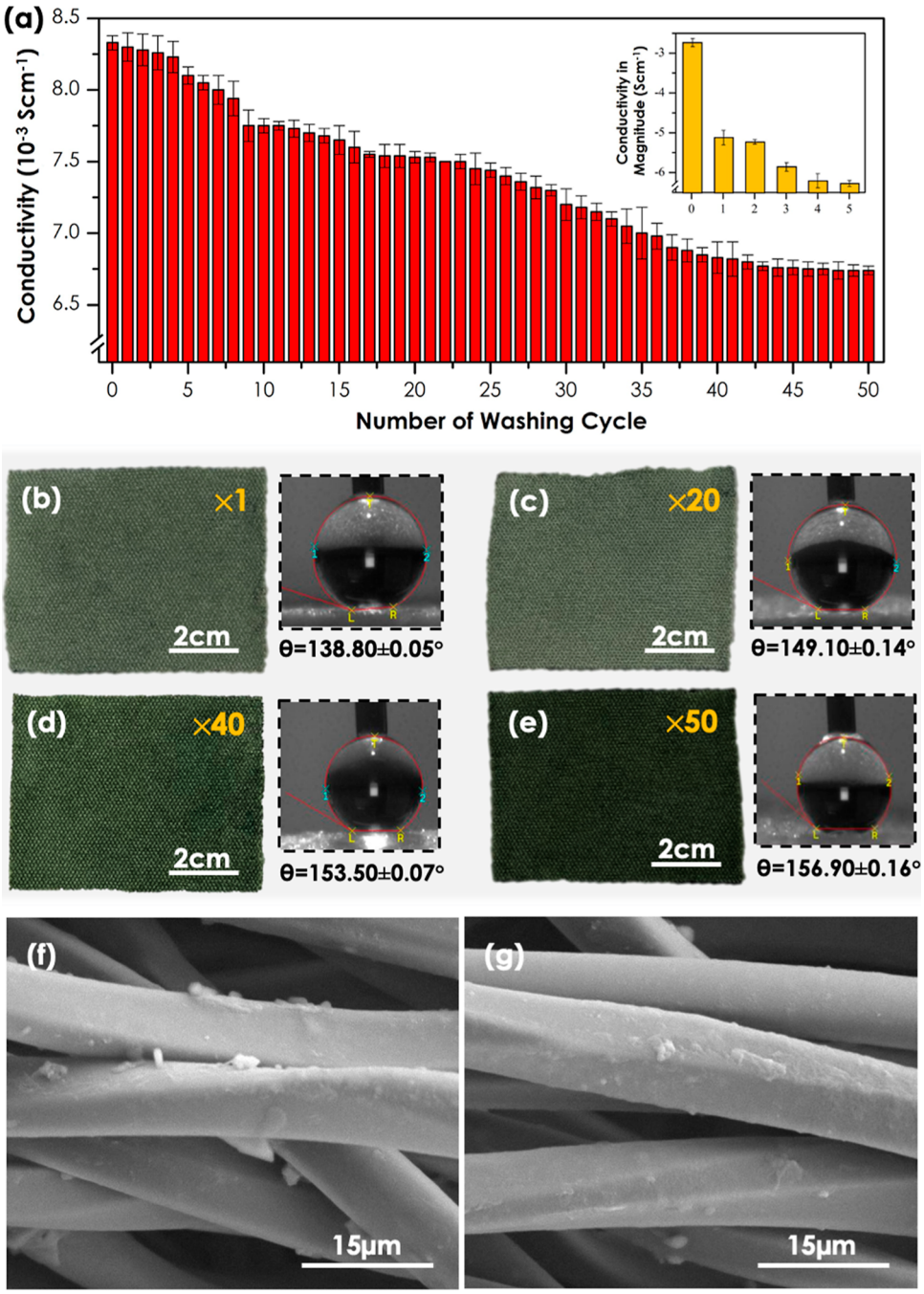

Figure 4. (a) Electrical conductivity of the PAA−PANI textile in each washing cycle. The inset figure is the conductivity of the PANI textile in five washing cycles (Table S2). The physical appearance of PAA−PANI textiles and their wettability angle in (b) 1st cycle, (c) 20th cycle, (d) 40th cycle, and (e) 50th cycle of washing. The SEM micrographs of the PAA−PANI textile in the (f) initial (1st cycle) and (g) final (50th cycle) of washing. Images were captured in 600× magnification.

of polymer chains. However, the cross-linking of PAA with PANI fibers led to a layer of PAA on the surface of PANI fibers. This PAA coverage produced a unique, fluid-like morphology. The carboxylic group was introduced to the fibers as previously described in FTIR analysis. The elemental compositions of carbon (C), sulfur (S), and oxygen (O) were measured on the PAA−PANI textile to validate the presence of the carboxylic group. The EDX mapping analysis is presented in the inset of Figure 3g and h. The C and O contents increased by 7.58 and 6.98% from the PANI fibers, respectively. These changes indicated total grafting of PAA on the textile. The distribution of these elements is presented in Figure S4.

3.2. Washing Evaluation of the PAA−PANI Textile. Washing evaluation measures the ability of the PAA−PANI textile to retain its electrical conductivity after repeated washings.[32] In this study, the reliability and lifespan of the PAA−PANI textile were evaluated in terms of ability of the textile to retain its conductivity upon washing. About 50 washing cycles of the PAA−PANI textile were performed, and the outcome of the PAA−PANI textile conductivity after washing is presented in Figure 4a. The data are tabulated in

https://doi.org/10.1021/acsomega.3c09871
ACS Omega 2024, 9, 23303−23315

Table 3. Comparison of Conductive Coating Integrated Textiles with Their Conductivity after Washing

conductive coating integrated textile	electrical conductivity/ resistivity (S/cm)	condition after washing evaluation	refs
polyester−PANI−cross-linked PAA	6.70−8.30 × 10^{-3}	stable and maintains a similar order of magnitude after 50 washing cycles	this work
cotton−reduced graphene oxide−polyurethane	∼6.25 × 10^{-7}	stable at a similar value after 5 washing cycles separately with cold and hot water	Olivieri et al.[35]
cotton−reduced graphene oxide−copper	0.5	copper decreased by 10% after 10 washing cycles	Chen et al.[36]
polyester−carbon nanotubes−chitosan−glucaric acid	∼8.70	conductivity decreased by 17% after 20 washing cycles	Zhu et al.[37]
polyester−reduced graphene oxide−phosphate	∼2 × 10^{-3}	conductivity dropped 24 times after 20 washing cycles	Zhao et al.[38]
cotton−reduced graphene oxide−polyurethane	3.33 × 10^{-4}	performance decreased by ∼10% after 10 washing cycles	Wang et al.[39]
cotton−reduced graphene oxide−carbon nanotubes	N/A	stable response after 10 washing cycles	Kim et al.[40]
cotton−PANI−polyglycidyl methacrylate-4-aminophenethylamine	∼9.26 × 10^{-3}	stable conductivity after 40 washing cycles	Wu et al.[41]

Table S1. Nevertheless, the decrease in conductivity from 8.30 ± 0.10 to 7.75 ± 0.05 × 10^{-3} S/cm from the 1st to 10th washing cycles could be attributed to the loss of PAA coating due to incomplete cross-linking. This result aligned with the finding from a reported study.[33] The significant conductivity drop of the PAA−PANI textile between the 11th and 42nd cycle from 7.75 ± 0.03 to 6.80 ± 0.05 × 10^{-3} S/cm could be attributed to several factors. The progressive deterioration of the PAA layer instigated a partial disintegration of PANI from the textile, potentially contributing to the reduced electrical conductivity. Moreover, the absence of robust covalent bonds between PAA and PANI might have interrupted the electronic network pathways, causing further conductivity deterioration.[34] However, the conductivity of the PAA−PANI textile began to stabilize around 6.70 × 10^{-3} S/cm, which took place between the 43rd and 50th cycles. This conductivity value implied the electrical stability of the textile over an extended period of use. One factor that could lead to this stability was the partial dissolution of PANI and PAA coating degradation from the textile during the initial washing cycles, which inevitably accelerated a state of equilibrium. The absence of notable fluctuations in conductivity measurements throughout the subsequent cycles insinuated that the residual PANI within the textile had preserved its conductive attributes, remaining impervious to further deterioration. Moreover, the residual PANI tenaciously adhered to the fibers, establishing an enduring lattice of electroconductive pathways. It is worth mentioning that incorporation of PAA into the PANI textile is able to reduce the probability of the conductive textile to lose its conductive properties as it is able to maintain conductivity at same order of magnitude (10^{-3} S/cm) throughout 50 washing cycles. This can be considered as a major improvement in terms of washing durability compared to that of pristine PANI textile (inset Figure 4a), which suffered declining conductivity over 4 orders of magnitude from 3.33 × 10^{-3} to 6.12 × 10^{-7} S/cm in only five washing cycles. The lack of resistance to the leaching of PANI from the textile contributed to its limited durability when subjected to the mechanical motion of washing. Fortunately, the incorporation of PAA bolstered the conductive network, enabling it to endure the rigors of the washing procedure. This evidence underlined the credibility of cross-linked PAA−PANI to realize stable conductive textiles. Structural confirmation and thermogram analysis of PAA−PANI textiles during washing evaluation are detailed in Figure S5. According to the records, this study extended the electrical durability of functional textiles, which could last up to 50 washing cycles (Table 3).

The physical appearance of the PANI−PAA textiles with their wettability angle during the washing cycles is illustrated in Figure 4b−e. According to Fujisaki et al.,[42] the green color signified the emeraldine salt form of PANI, which was responsible for its conductive properties. After a washing cycle, the color of the PANI textile may change to blue (emeraldine base state), providing an initial indication of its insulating properties.[43] Nonetheless, the PAA−PANI textile remained unchanged in color and conductivity after 50 washing cycles. However, the darkening of the textile after 20, 40, and 50 washing cycles insinuated a loss of the PAA−PANI component. As stated by Anastasiia et al., PANI exhibits high electrical conductivity in its fully oxidized (emeraldine salt) state.[44] Nonetheless, the electrical conductivity of PANI can be greatly influenced when it undergoes oxidation or reduction processes. In this case, the washing cycles could promote a reduced state, leading to a diminishing conductivity. Despite undergoing repeated washing cycles, the PAA−PANI textile demonstrated green-color stability overall. However, it undergoes a slight color transition upon washing, which could be an indicator that the component in PAA−PANI experienced some degradation.

Since moisture absorption is critical for textile comfort, further investigation was performed to evaluate the wettability of the PAA−PANI textile. The wettability angle of the textile after the first washing cycle was 138.8 ± 0.05°, followed by 149.10 ± 0.14, 153.50 ± 0.07, and 156.90 ± 0.16° after 20, 40, and 50 washing cycles, respectively. In the initial cycle, the layer of PAA on the PANI textile was intact, which lent some degree of hydrophobicity to the surface. As the textile progressed further in subsequent washing cycles, the PAA coating was eroded from the textile surface. This erosion promoted a rough surface area. Koch et al. asserted that these conditions would reduce the wetting and surface tension of the surface by liquid detergent.[45] Repeated washing cycles could alter a surface's chemical composition and physical structure. For example, the surface may become rougher or porous due to mechanical abrasion or loss of PAA segments. As a result, the contact angle would become greater, since the rough or porous surface would have more air pockets that could trap air and reduce wetting. The higher hydrophobicity of the PAA−PANI textile could also influence its conductivity. Moisture on the textile surface could interfere with the flow of the electric

https://doi.org/10.1021/acsomega.3c09871
ACS Omega 2024, 9, 23303−23315

current. Water and detergent acted as a barrier between the conductive pathways in the textile, reducing the current flow's efficiency and giving off lower conductivity.[46]

Figure 4f,g illustrates SEM micrographs of the PAA−PANI textile in the first and final (50th) cycles of washing. Despite the disintegration of PAA and PANI from the textile, the homogeneous surface structure was intact. This work demonstrated that chemical cross-linking between the PES fabric and PAA improved the durability against multiple washing cycles and thus was able to preserve the conductivity properties of the textile.

3.3. Antibacterial Evaluation of the PAA−PANI Textile. The 30% PAA−PANI textile was selected for antibacterial assessment due to its excellent electrical conductivity with moderate mechanical properties. The antibacterial efficacy of this textile was studied against Gram-positive bacterium, *S. aureus,* and Gram-negative bacterium, *P. aeruginosa.* These pathogens carry a risk of bacterial transmission in wearable textiles. The inhibition zone on the bacterial disk around PANI and PAA−PANI textiles was observed after 18 h of incubation. As seen in Figure 5a,b, the inhibition zone was absent on the pristine PES textile. In contrast, introducing PAA−PANI into the pristine textile yielded a transparent inhibition zone that implied antibacterial properties against the selected bacteria. The details of the inhibition zone around the surface of textiles are recorded in Table 4.

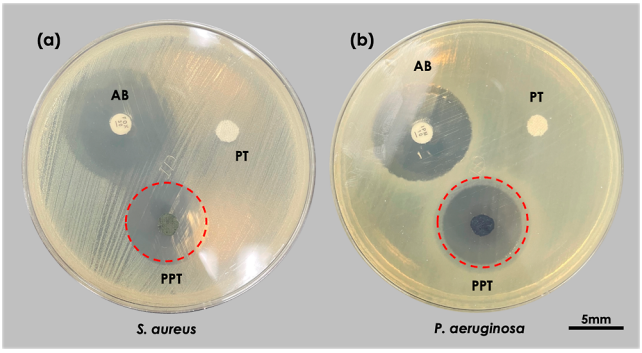

Figure 5. Disc diffusion assays of the PAA−PANI textile, PANI textile, antibiotic (AB)-positive control and PES textile (PT)-negative control against (a) *S. aureus* and (b) *P. aeruginosa*.

Table 4. Diameter of the Inhibition Zone around PAA−PANI and Pristine PES Textiles in Contact with *S. aureus* and *P. aeruginosa*

bacteria	textile	inhibition zone (mm)
S. aureus (ATCC25923)	PT	NIL
	PAA−PANI	15.5 ± 0.09
P. aeruginosa (ATCC27853)	PT	NIL
	PAA−PANI	17.0 ± 0.04

In principle, the PANI textile in protonated state could exhibit remarkable antibacterial activity against bacteria. Our previous findings showed that the PANI textile had mean inhibition zone sizes of ∼22.30 ± 0.03 mm and ∼24.33 ± 0.02 mm against *S. aureus* and *P. aeruginosa*, respectively.[10] The acid dopants in the textile were responsible for these inhibition zones and antibacterial activity. As the protonating dopant leached out over time, the textile's surface inhibited the growth of several bacterial isolates. These findings were consistent with numerous reports on PANI's antibacterial properties.[47−49] The decline in antibacterial effectiveness over time can be attributed to excessive leaching of the dopant. The transformation from green to blue after incubation hinted at the deprotonation of PANI.

In contrast, PAA−PANI exhibited smaller inhibition zones than those of PANI textile against *S. aureus* and *P. aeruginosa*, with mean sizes of 15.5 ± 0.09 and 12.3 ± 0.04 mm, respectively. The presence of PAA in the PANI textile slowed the release of antimicrobial agents and the diffusion of protonated PANI from the textile. These properties secured the antibacterial efficacy of the PAA−PANI textile after multiple washing cycles. Additional research was conducted to examine the long-lasting antibacterial properties of the PAA−PANI fabric after 50 washing cycles.

3.4. Antibacterial Durability of the PAA−PANI Textile. The antimicrobial durability of the PAA−PANI textile after 50 washing cycles was evaluated by analyzing the inhibition zone on MH agar, as presented in Figure 6. The corresponding data are tabulated in Table S3. Examination of the inhibition zone suggested that the PAA−PANI textile inhibited the growth of *S. aureus* and *P. aeruginosa* after 50 washing cycles. This durability was proof that mechanical scouring in washing would not disrupt the textile's efficacy in the long run. Moreover, the effectiveness rate of PAA−PANI textiles in killing bacteria was recorded in Table 5.

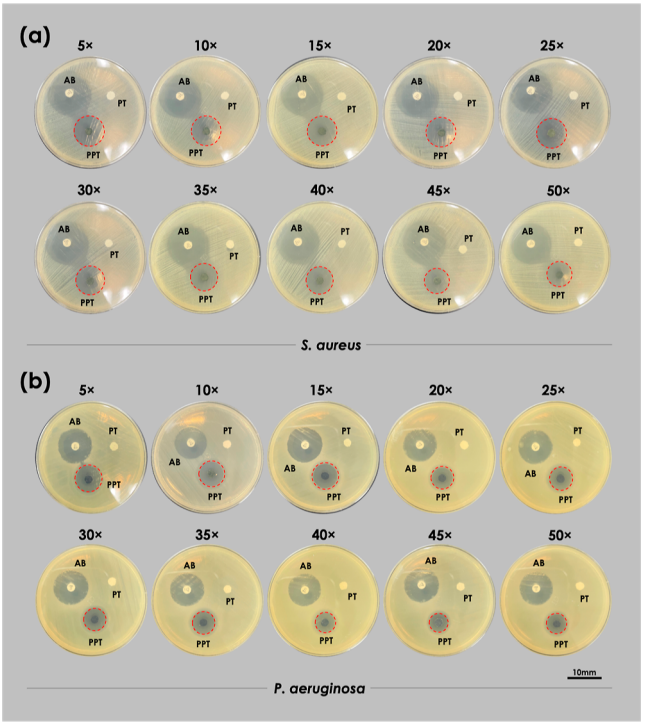

Figure 6. Inhibition zone revealed by the PAA−PANI textile (PPT), PES textile (PT)-negative control, and antibiotic (AB)-positive control against (a) *S. aureus* and (b) *P. aeruginosa* in 50 washing cycles.

The prewashing antibacterial effectiveness of the PAA−PANI textile was pegged at 99.99% for both strains. This value gradually dropped to 95.48% for *S. aureus* and 92.35% for *P. aeruginosa* after 50 washing cycles. The excellent antibacterial

https://doi.org/10.1021/acsomega.3c09871
ACS Omega 2024, 9, 23303−23315

Table 5. Antibacterial Effectiveness Rate of the PAA−PANI Textile against *S. aureus* and *P. aeruginosa* in Each Washing Cycle

	antibacterial effectiveness (%)	
number of washing cycle	*S. aureus*	*P. aeruginosa*
without washing	99.99	99.99
5	99.35	95.88
10	99.35	95.88
15	98.03	96.47
20	98.03	96.47
25	96.77	94.12
30	96.77	94.71
35	96.77	97.06
40	97.42	96.47
45	96.77	94.12
50	95.48	92.35

retention of the PAA−PANI textile at above 90% effectiveness could be attributed to the carboxylic groups in the PANI backbone. These groups covalently reacted with the hydroxyl groups on the textile surface. This reaction prevented the dissolution and subsequent loss of polymers in washing cycles without losing their antibacterial release behavior.

The present study indicated a superior antibacterial ability of PAA−PANI against *S. aureus* than against *P. aeruginosa*. *S. aureus* possesses a thicker peptidoglycan layer in its cell wall. This characteristic reinforces its resistance to damage by antimicrobial agents.[50,51] According to Painter et al., the lower resistance of *S. aureus* to oxidative stress makes it more vulnerable to antimicrobial agents like PAA−PANI.[52] Conversely, *P. aeruginosa* possesses an outer membrane that provides resistance to antimicrobial substances such as antibiotics and disinfectants. This outer membrane prevents the PAA−PANI antimicrobial agent from penetrating the cell, which can reduce its effectiveness.[53] Additionally, *P. aeruginosa* is recognized for generating various virulence factors and

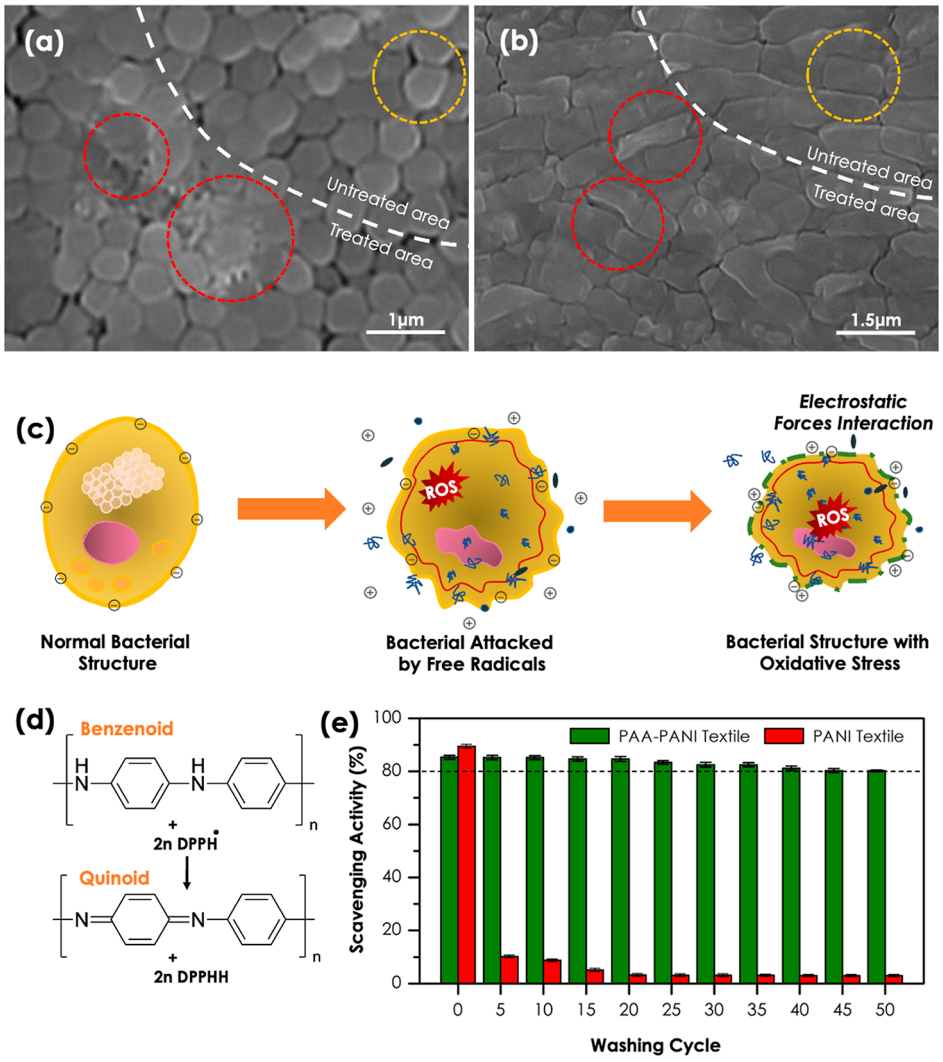

Figure 7. SEM images of (a) *S. aureus* and (b) *P. aeruginosa* on the untreated and treated area on the disk diffusion assay (see Figure S3 for a disk reference). Orange and red circles indicate normal cell structure and membrane disruption, respectively. Images were captured at 12,000× and 30,000× magnifications. (c) Two potential antibacterial mechanisms of the PAA−PANI textile: electrostatic interaction between the textile's cationic compounds and the anionic charges in the bacterial membrane, as well as the byproduct of hydroxyl radicals from the reaction of PANI with the atmosphere. (d) Conversion of the chemical structure of PANI's benzenoid units to quinoid units leads to the quenching of the DPPH radical. (e) Scavenging activity of PAA−PANI and PANI textiles through 50 washing cycles.

https://doi.org/10.1021/acsomega.3c09871
ACS Omega 2024, 9, 23303−23315

exopolysaccharides, which enhance its capability to adapt to diverse environments and withstand antimicrobial substances. These factors might contribute to diminishing the efficiency of the PAA−PANI antimicrobial agent in combating *P. aeruginosa*.

The antibacterial efficiency of the textile was assessed by examining the morphological alterations in the bacteria. Figure 7a,b presents the SEM images of untreated *S. aureus* and *P. aeruginosa* bacterial cells, respectively. In these images, the untreated areas (marked by orange circles) exhibit a smooth and intact surface, which suggests that the normal structures of these bacteria are preserved. However, the images of the treated bacteria (red circles in a similar image) revealed morphological changes, such as membrane corrugations due to wrinkling and damage. These changes confirmed the role of the PAA−PANI textile in disrupting the bacterial cell membrane. Additionally, deformations and perforations indicative of cell wall disruption were evident in some parts of the cell due to deformations and perforations.[54,55] The combination of rough surface, protruding fibers in morphological images, and elemental mapping distribution after bacteria exposure suggested successful antibacterial actions of PAA−PANI (Figure S6 and Table S4).

Further evidence has strengthened the belief that the PAA−PANI textile possessed antibacterial properties. The antibacterial mechanism of PAA−PANI necessitated multiple pathways, including the generation of reactive oxygen species (ROS) and the disruption of bacterial cell membranes (Figure 7c). The presence of hydroxyl radicals from the synthesis of hydrogen peroxide by PANI from the textile into the surrounding atmosphere may facilitate the disruption of bacterial cell membranes. The treated textile emitted ROS that interfered with various biological reactions and damaged the bacterial membrane. As reported by Vaishampayan et al., ROS could react with bacterial DNA, causing genetic damage and inhibiting bacterial growth and replication.[56]

PAA in the PAA−PANI textile could also interact with bacterial cell membranes, leading to membrane destabilization and leakage of cellular contents.[57,58] The negatively charged carboxyl groups in PAA interacted with positively charged molecules on the bacterial surface, destabilizing the membrane structure. As a result, the leakage of essential cellular components can kill the bacteria.

The synergy of both antibacterial agents in the PAA−PANI textile augmented antibacterial activity more than the actions of individual polymers alone. The functional PAA binder in PAA−PANI facilitated the adsorption of PANI onto the textile surface. The increased concentration of PANI promoted the generation of ROS and stimulated the disruption of the bacterial cell membranes. All of these actions contributed to an efficient antibacterial property.

In the PAA−PANI textile, PANI played a crucial role in the scavenging of ROS. The scavenging activity was demonstrated through the hydrogen release of PANI. Previous studies have shown that reduced (benzenoid) units of PANI could be oxidized by DPPH radicals,[59,60] as depicted in Figure 7d. This process required the conversion of the benzenoid units of PANI to quinoid units. The quenching of the DPPH radical was the outcome of this conversion. Therefore, a higher proportion of benzenoid units can scavenge more DPPH to exhibit superior antioxidant activity.

Figure 7e distinguishes the scavenging activity of the PAA−PANI textile and PANI textile in 50 cycles of washing. The scavenging activity of the PANI textile deteriorated from the 1st to the 20th cycle of washing, inasmuch as from 89.44 to 3.22%. This activity proceeded to drop steadily until the final washing cycle. This finding suggested a low affinity of PANI's benzenoid unit to textile during washing. On the other hand, the scavenging activity of the PAA−PANI textile dropped from 85.30 to 80% over 50 cycles of washing. Even though the PANI segments were firmly attached to the PAA-cross-linked textile, PANI was gradually released during washing. Overall, it was postulated that the PAA−PANI textile could continuously supply antioxidant activity for sustainable release.

4. CONCLUSIONS

This study elucidates the development of highly durable antibacterial textiles through the cross-linking of PAA onto a PANI textile. The resultant hybrid PAA−PANI textile exhibits notable electrical conductivity, measuring $8.33 \pm 0.04 \times 10^{-3}$ S/cm when cross-linked with 30% PAA, which falls within the semiconductor range of polymeric materials. Beyond assessing electrical conductivity, the study emphasizes the importance of evaluating durability and material integrity in washing assessments for functional textiles. Notably, the PANI−PAA textile demonstrates prolonged electrical stability within a similar order of magnitude (10^{-3} S/cm) even after 50 washing cycles, while the pristine PANI textile experiences a drastic decline in conductivity over just five cycles, diminishing by 4 orders of magnitude from 3.33×10^{-3} to 6.12×10^{-7} S/cm. Moreover, the study evaluates the antibacterial durability of the functional PANI−PAA textile to ascertain its long-term efficacy against bacteria. The PAA−PANI textile exhibits outstanding antibacterial durability, retaining 95.48 and 92.35% efficacy against *P. aeruginosa* and *S. aureus*, respectively, even after 50 washing cycles. Furthermore, the textile demonstrates a scavenging activity of up to 80%, suggesting sustainable release of antioxidants. The observed integrity of the textile materials underscores their long-term antibacterial properties, positioning them for practical applications. These findings offer promising solutions for combating infectious diseases and highlight the potential utility of these textiles in real-world scenarios.

■ ASSOCIATED CONTENT

Supporting Information

The Supporting Information is available free of charge at https://pubs.acs.org/doi/10.1021/acsomega.3c09871.

Conductivity trends of protonated PANI textiles at different concentrations of *p*TSA with their respective values; tensile test of PAA-PANI textile using Tenso Lab strength tester; illustration of Kirby disk diffusion assay after being treated to textile samples; SEM images and elemental mapping of PANI textile and PAA-PANI textile; conductivity values of PAA-PANI textile in different washing cycles; conductivity values of PANI textile in 5 washing cycles; inhibition zone formed around PAA-PANI textiles against *S. aureus* and *P. aeruginosa* in different washing cycles; IR spectra of PAA-PANI textiles undergoing 20 cycle and 50 cycle washing evaluations; SEM images and elemental mapping of treated PAA-PANI textile against *S. aureus* and *P. aeruginosa* in 25 and 50 cycles of washing; and elemental compositions of treated PAA-PANI textile

https://doi.org/10.1021/acsomega.3c09871
ACS Omega 2024, 9, 23303−23315

against *S. aureus* and *P. aeruginosa* in 25 cycles and 50 cycles of washing (PDF)

AUTHOR INFORMATION

Corresponding Authors

Muhammad Faiz Aizamddin − *Group Research and Technology, PETRONAS Research Sdn. Bhd., 43000 Selangor, Malaysia; School of Physics and Material Studies, Faculty of Applied Sciences, Universiti Teknologi MARA, Shah Alam 40450, Malaysia;* orcid.org/0009-0001-6095-5322; Email: faiz.aizamddin@petronas.com

Maung Maung Myo Thant − *Group Research and Technology, PETRONAS Research Sdn. Bhd., 43000 Selangor, Malaysia*; Email: maungmyothant@petronas.com

Mohd Muzamir Mahat − *School of Physics and Material Studies, Faculty of Applied Sciences, Universiti Teknologi MARA, Shah Alam 40450, Malaysia; Textile Research Group, Faculty of Applied Sciences, Universiti Teknologi MARA, Shah Alam 40450, Malaysia;* orcid.org/0000-0002-2448-3241; Email: mmuzamir@uitm.edu.my

Authors

Zaidah Zainal Ariffin − *School of Biology, Faculty of Applied Sciences, Universiti Teknologi MARA, Shah Alam 40450, Malaysia*

Nur Asyura Nor Amdan − *Bacteriology Unit, Infectious Disease Research Centre, Institute for Medical Research, National Institutes of Health, Shah Alam 40170, Malaysia*

Mohd Azizi Nawawi − *School of Chemistry and Environment, Faculty of Applied Sciences, Universiti Teknologi MARA, Shah Alam, Selangor 40450, Malaysia*

Nur Aimi Jani − *School of Physics and Material Studies, Faculty of Applied Sciences, Universiti Teknologi MARA, Shah Alam 40450, Malaysia;* orcid.org/0000-0002-8659-3171

Muhd Fauzi Safian − *School of Chemistry and Environment, Faculty of Applied Sciences, Universiti Teknologi MARA, Shah Alam, Selangor 40450, Malaysia*

Siti Nur Amira Shaffee − *Group Research and Technology, PETRONAS Research Sdn. Bhd., 43000 Selangor, Malaysia*

Nik Mohd Radi Nik Mohamed Daud − *Group Research and Technology, PETRONAS Research Sdn. Bhd., 43000 Selangor, Malaysia*

Complete contact information is available at: https://pubs.acs.org/10.1021/acsomega.3c09871

Author Contributions

M.F.A. and M.M.M.: conceptualization, methodology, investigation (polymerization, fabrication, and all other studies), visualization, and original draft preparation. M.F.A., M.M.M., N.A.N.A., and N.A.J.: methodology, reviewing, and editing. Z.Z.A.: supervision, reviewing, and editing. M.M.M., M.M.M.T., S.N.A.S., M.F.S., N.M.R.N.M.D., and M.A.N.: supervision, reviewing, editing, and funding acquisition. All authors have read and agreed to the published version of the manuscript.

Funding

This work was funded by PETRONAS through PETRONAS Research Sdn. Bhd., under project code E.025.ENERGY.00001.009.

Notes

The authors declare no competing financial interest.

ACKNOWLEDGMENTS

This work was funded by PETRONAS through PETRONAS Research Sdn. Bhd., under project code E.025.ENERGY.00001.009. A special thanks is extended to Dayangku Nurshahidah Nafesah Abd Adzim for her assistance with the laboratory work and guidance in the antibacterial research.

REFERENCES

(1) Iqbal, S. M. A.; Mahgoub, I.; Du, E.; Leavitt, M. A.; Asghar, W. Advances in Healthcare Wearable Devices. *npj Flexible Electron.* **2021**, *5* (1), 9.

(2) Ferguson, T.; Olds, T.; Curtis, R.; Blake, H.; Crozier, A. J.; Dankiw, K.; Dumuid, D.; Kasai, D.; O'Connor, E.; Virgara, R.; Maher, C. Effectiveness of Wearable Activity Trackers to Increase Physical Activity and Improve Health: A Systematic Review of Systematic Reviews and Meta-Analyses. *Lancet Digital Health* **2022**, *4* (8), 615−626.

(3) Schneider, G.; Bim, F. L.; Sousa, Á. F. L. d.; Watanabe, E.; Andrade, D. d.; Fronteira, I. The Use of Antimicrobial-Impregnated Fabrics in Health Services: An Integrative Review. *Rev. Lat. Am. Enfermagem* **2021**, *29*, 3416.

(4) Rashid, M. M.; Simončič, B.; Tomšič, B. Recent advances in TiO2-functionalized textile surfaces. *Surf. Interfaces* **2021**, *22*, 100890.

(5) Aizamddin, M. F.; Mahat, M. M.; Zainal Ariffin, Z. Z.; Samsudin, I.; Razali, M. S. M.; Amir, M. Synthesis, Characterisation and Antibacterial Properties of Silicone−Silver Thin Film for the Potential of Medical Device Applications. *Polymers* **2021**, *13* (21), 3822.

(6) Ilieş, A.; Hodor, N.; Pantea, E.; Ilieş, D. C.; Indrie, L.; Zdrîncă, M.; Iancu, S.; Caciora, T.; Chiriac, A.; Ghergheles, C.; Taghiyari, H. R.; Costea, M.; Baias, Ş. Antibacterial Effect of Eco-Friendly Silver Nanoparticles and Traditional Techniques on Aged Heritage Textile, Investigated by Dark-Field Microscopy. *Coatings* **2022**, *12* (11), 1688.

(7) Temizel-Sekeryan, S.; Hicks, A. L. Global Environmental Impacts of Silver Nanoparticle Production Methods Supported by Life Cycle Assessment. *Resour., Conserv. Recycl.* **2020**, *156*, 104676.

(8) Aizamddin, M. F.; Shaffee, S. N. A.; Halizan, M. Z. M.; Shafiee, S. A.; Sabere, A. S. M.; Sofian, Z. M.; Daud, N.; Bahrudin, F. I.; Harun, I.; Rahman, N. A.; Mahat, M. M. Utilizing Membrane Technologies in Advancing the Recycling of Spent Lithium-Ion Batteries Using Green Electrochemical Method—A Review. *Mater. Res. Proc.* **2023**, *29*, 170−191.

(9) Aizamddin, M. F.; Mahat, M. M.; Nawawi, M. A.; Jani, N. A.; Ariffin, Z. Z.; Yahya, S. Y. S. Electrical Conductivity and Thermal Stability of Conductive Polyaniline Fabric-Based Polyacrylonitrile Blends. *AIP Conf. Proc.* **2023**, *2720* (1), 040020.

(10) Aizamddin, M. F.; Mahat, M. M.; Zainal Ariffin, Z.; Nawawi, M. A.; Jani, N. A.; Nor Amdan, N. A.; Sadasivuni, K. K. Antibacterial Performance of Protonated Polyaniline-Integrated Polyester Fabrics. *Polymers* **2022**, *14*, 2617.

(11) Dhivya, C.; Vandarkuzhali, S. A. A.; Radha, N. Antimicrobial Activities of Nanostructured Polyanilines Doped with Aromatic Nitro Compounds. *Arabian J. Chem.* **2019**, *12* (8), 3785−3798.

(12) Omar, S. N. I.; Zainal Ariffin, Z.; Zakaria, A.; Safian, M. F.; Halim, M. I. A.; Ramli, R.; Sofian, Z. M.; Zulkifli, M. F.; Aizamddin, M. F.; Mahat, M. M. Electrically Conductive Fabric Coated with Polyaniline: Physicochemical Characterisation and Antibacterial Assessment. *Emergent Mater.* **2020**, *3*, 469−477.

(13) Maruthapandi, M.; Saravanan, A.; Gupta, A.; Luong, J. H. T.; Gedanken, A. Antimicrobial Activities of Conducting Polymers and Their Composites. *Macromolecules* **2022**, *2* (1), 78−99.

(14) Robertson, J.; Gizdavic-Nikolaidis, M.; Nieuwoudt, M. K.; Swift, S. The Antimicrobial Action of Polyaniline Involves Production of Oxidative Stress While Functionalisation of Polyaniline Introduces Additional Mechanisms. *PeerJ* **2018**, *6*, 5135.

(15) Erdem, R.; Rajendran, S. Influence of Silver Loaded Antibacterial Agent on Knitted and Nonwoven Fabrics and Some Fabric Properties. *J. Eng. Fibers Fabr.* **2016**, *11* (1), 155892501601100.
(16) Semnani, D.; Afrashi, M.; Alihosseini, F.; Dehghan, P.; Maherolnaghsh, M. Investigating the Performance of Drug Delivery System of Fluconazole Made of Nano-Micro Fibers Coated on Cotton/Polyester Fabric. *J. Mater. Sci.: Mater. Med.* **2017**, *28* (11), 175.
(17) Nabipour, H.; Wang, X.; Rahman, M. Z.; Song, L.; Hu, Y. An Environmentally Friendly Approach to Fabricating Flame Retardant, Antibacterial and Antifungal Cotton Fabrics via Self-Assembly of Guanazole-Metal Complex. *J. Cleaner Prod.* **2020**, *273*, 122832.
(18) Qiu, H.; Si, Z.; Luo, Y.; Feng, P.; Wu, X.; Hou, W.; Zhu, Y.; Chan-Park, M. B.; Xu, L.; Huang, D. The Mechanisms and the Applications of Antibacterial Polymers in Surface Modification on Medical Devices. *Front. Bioeng. Biotechnol.* **2020**, *8*, 910.
(19) Maliszewska, I.; Czapka, T. Electrospun Polymer Nanofibers with Antimicrobial Activity. *Polymers* **2022**, *14* (9), 1661.
(20) Luo, Y.; Liu, Z.; Wang, L.; Zhao, X.; Li, H.; Wu, M. High Antibacterial and Antioxidant Cotton Fabric Based on AgNPs@ HTCS and Hyaluronic Acid via Lay by Lay Self-Assembly. *J. Ind. Text.* **2022**, *52*, 152808372211409.
(21) Aizamddin, M. F.; Mahat, M. M.; Roslan, N. C.; Adila, D.; Ruzaidi, A.; Ayub, A. N. Techniques for Designing Patterned Conducting Polymers. *Conjugated Polymers for Next-Generation Applications*; Woodhead Publishing, 2022; Vo. *1*, pp 39−77.
(22) Roslan, N. C.; Aizamddin, M. F.; Adila, D.; Ruzaidi, A.; Ayub, A. N.; Ain, N.; Asri, N.; Jani, N. A.; Shafiee, S. A.; Mahat, M. M. Conducting Polymer-Based Textile Materials. *Conducting Polymer-Based Energy Storage Materials*; Woodhead Publishing, 2022; Vol. *1*, pp 325−359.
(23) Qiu, Q.; Chen, S.; Li, Y.; Yang, Y.; Zhang, H.; Quan, Z.; Qin, X.; Wang, R.; Yu, J. Functional Nanofibers Embedded into Textiles for Durable Antibacterial Properties. *Chem. Eng. J.* **2020**, *384*, 123241.
(24) Hassan, M. M. Wash-Durability, Surface, and Antibacterial Properties of Wool Fabric Treated with Nature-Derived Thymol and Totarol under Subcritical CO2, Aqueous, and Ethanol Media. *Process Saf. Environ. Prot.* **2023**, *177*, 355−365.
(25) Aizamddin, M. F.; Saaid, F. I.; Zakaria, P. N. M.; Mahat, M. M. Revealing the Effects of Various Acid Dopants on the Electrical Conductivity and Electrochemical Activity of Conductive Polyaniline Fabrics. *AIP Conf. Proc.* **2023**, *2983*, 020001.
(26) Ayub, A. N.; Ismail, N. A.; Aizamddin, M. F.; Bonnia, N. N.; Sulaiman, N. S.; Nadzri, N. I. M.; Mahat, M. M. Effects of Organic Solvent Doping on the Structural and Conductivity Properties of PEDOT: PSS Fabric. *J. Phys.: Conf. Ser.* **2022**, *4*, 012008.
(27) Mahat, M. M.; Aizamddin, M. F.; Roslan, N. C.; Kamarudin, M. A.; Nurzatul, S.; Omar, I.; Mazo, M. M. Conductivity, Morphology and Thermal Studies of Polyaniline Fabrics. *J. Mech. Eng.* **2020**, *9* (1), 137−150.
(28) Aizamddin, M. F.; Mahat, M. M. Enhancing the Washing Durability and Electrical Longevity of Conductive Polyaniline-Grafted Polyester Fabrics. *ACS Omega* **2023**, *8*, 37936−37947.
(29) Aizamddin, M. F.; Mahat, M. M.; Nawawi, M. A. Morphological, Structural and Electrochemical Studies of Conductive Polyaniline Coated Polyester Fabrics. *Int. Exc. Inn. Conf. Eng. Sci.* **2019**, *5*, 53−57.
(30) Namsheer, K.; Rout, C. S. Conducting Polymers: A Comprehensive Review on Recent Advances in Synthesis, Properties and Applications. *RSC Adv.* **2021**, *11* (10), 5659−5697.
(31) Bagheri, N.; Mansour Lakouraj, M.; Nabavi, S. R.; Tashakkorian, H.; Mohseni, M. Synthesis of Bioactive Polyaniline-b-Polyacrylic Acid Copolymer Nanofibrils as an Effective Antibacterial and Anticancer Agent in Cancer Therapy, Especially for HT29 Treatment. *RSC Adv.* **2020**, *10* (42), 25290−25304.
(32) Ullah, S.; Iftikhar Ahmed, H.; Ali Hamdani, S. T. Effect of Washing and Temperature on Electrical Properties of Conductive Yarns and Woven Fabrics. *Ind. Text.* **2022**, *73* (01), 34−39.
(33) Kaewsaneha, C.; Elaissari, A.; Tangboriboonrat, P.; Opaprakasit, P. Self-Assembly of Amphiphilic Poly(Styrene-: B -Acrylic Acid) on Magnetic Latex Particles and Their Application as a Reusable Scale Inhibitor. *RSC Adv.* **2020**, *10* (67), 41187−41196.
(34) Beygisangchin, M.; Abdul Rashid, S.; Shafie, S.; Sadrolhosseini, A. R. Polyaniline Synthesized by Different Dopants for Fluorene Detection via Photoluminescence Spectroscopy. *Materials* **2021**, *14* (23), 7382.
(35) Olivieri, F.; Rollo, G.; De Falco, F.; Avolio, R.; Bonadies, I.; Castaldo, R.; Cocca, M.; Errico, M. E.; Lavorgna, M.; Gentile, G. Reduced Graphene Oxide/Polyurethane Coatings for Wash-Durable Wearable Piezoresistive Sensors. *Cellulose* **2023**, *30*, 2667−2686.
(36) Chen, F.; Liu, H.; Xu, M.; Ye, J.; Li, Z.; Qin, L.; Zhang, T. Flexible Cotton Fabric with Stable Conductive Coatings for Piezoresistive Sensors. *Cellulose* **2021**, *28* (15), 10025−10038.
(37) Zhu, S.; Wang, M.; Qiang, Z.; Song, J.; Wang, Y.; Fan, Y.; You, Z.; Liao, Y.; Zhu, M.; Ye, C. Multi-Functional and Highly Conductive Textiles with Ultra-High Durability through 'Green' Fabrication Process. *Chem. Eng. J.* **2021**, *406*, 127140.
(38) Zhao, Y.; Wang, J.; Li, Z.; Zhang, X.; Tian, M.; Zhang, X.; Liu, X.; Qu, L.; Zhu, S. Washable, Durable and Flame Retardant Conductive Textiles Based on Reduced Graphene Oxide Modification. *Cellulose* **2020**, *27* (3), 1763−1771.
(39) Wang, Y.; Wang, W.; Xu, R.; Zhu, M.; Yu, D. Flexible, Durable and Thermal Conducting Thiol-Modified RGO-WPU/Cotton Fabric for Robust Electromagnetic Interference Shielding. *Chem. Eng. J.* **2019**, *360*, 817−828.
(40) Kim, S. J.; Song, W.; Yi, Y.; Min, B. K.; Mondal, S.; An, K. S.; Choi, C. G. High Durability and Waterproofing RGO/SWCNT-Fabric-Based Multifunctional Sensors for Human-Motion Detection. *ACS Appl. Mater. Interfaces* **2018**, *10* (4), 3921−3928.
(41) Wu, B.; Zhang, B.; Wu, J.; Wang, Z.; Ma, H.; Yu, M.; Li, L.; Li, J. Electrical Switchability and Dry-Wash Durability of Conductive Textiles. *Sci. Rep.* **2015**, *5*, 11255.
(42) Fujisaki, T.; Kashima, K.; Serrano-Luginbühl, S.; Kissner, R.; Bajuk-Bogdanović, D.; Milojević-Rakić, M.; Ćirić-Marjanović, G.; Busato, S.; Lizundia, E.; Walde, P. Effect of Template Type on the Preparation of the Emeraldine Salt Form of Polyaniline (PANI-ES) with Horseradish Peroxidase Isoenzyme C (HRPC) and Hydrogen Peroxide. *RSC Adv.* **2019**, *9* (57), 33080−33095.
(43) Aizamddin, M. F.; Roslan, N. C.; Kamarudin, M. A.; Omar, S. N. I.; Safian, M. F.; Halim, M. I. A.; Mahat, M. M. Study of Conductivity and Thermal Properties of Polyaniline Doped with P-Toluene Sulfonic Acid. *Malays. J. Anal. Sci.* **2020**, *24* (3), 413−421.
(44) Andriianova, A. N.; Biglova, Y. N.; Mustafin, A. G. Effect of Structural Factors on the Physicochemical Properties of Functionalized Polyanilines. *RSC Adv.* **2020**, *10* (13), 7468−7491.
(45) Koch, B. M. L.; Amirfazli, A.; Elliott, J. A. W. Wetting of Rough Surfaces by a Low Surface Tension Liquid. *J. Phys. Chem. C* **2014**, *118* (41), 23777−23782.
(46) Sun, M.; Wang, X.; Winter, L. R.; Zhao, Y.; Ma, W.; Hedtke, T.; Kim, J.-H.; Elimelech, M. Electrified Membranes for Water Treatment Applications. *ACS ES&T Eng.* **2021**, *1* (4), 725−752.
(47) Ren, Y.; Yan, B.; Lin, C.; Wang, P.; Zhou, M.; Cui, L.; Yu, Y.; Wang, Q. Multifunctional Textile Constructed via Polyaniline-Mediated Copper Sulfide Nanoparticle Growth for Rapid Photothermal Antibacterial and Antioxidation Applications. *ACS Appl. Nano Mater.* **2023**, *6*, 1212−1223.
(48) Jarach, N.; Meridor, D.; Buzhor, M.; Raichman, D.; Dodiuk, H.; Kenig, S.; Amir, E. Hybrid Antibacterial and Electro-Conductive Coating for Textiles Based on Cationic Conjugated Polymer. *Polymers* **2020**, *12* (7), 1517.
(49) Omar, S. N. I.; Ariffin, Z. Z.; Akhir, R. A. M.; Shri, D. N. A.; Halim, M. I. A.; Safian, M. F.; Azman, H. H.; Ramli, R.; Mahat, M. M. Polyaniline (PANI) fabric doped p-toluene sulfonic acid (pTSA) with anti-infection properties. *Mater. Today: Proc.* **2019**, *16*, 1994−2002.
(50) Wu, Y.; Yang, Y.; Zhang, Z.; Wang, Z.; Zhao, Y.; Sun, L. Fabrication of Cotton Fabrics with Durable Antibacterial Activities Finishing by Ag Nanoparticles. *Text. Res. J.* **2019**, *89* (5), 867−880.

https://doi.org/10.1021/acsomega.3c09871
ACS Omega 2024, 9, 23303−23315

(51) Mahat, M. M.; Sabere, A. S. M.; Azizi, J.; Amdan, N. A. N. Potential Applications of Conducting Polymers to Reduce Secondary Bacterial Infections among COVID-19 Patients: A Review. *Emergent Mater.* **2021**, *4*, 279−292.
(52) Painter, K. L.; Strange, E.; Parkhill, J.; Bamford, K. B.; Armstrong-James, D.; Edwards, A. M. Staphylococcus Aureus Adapts to Oxidative Stress by Producing H2O2-Resistant Small-Colony Variants via the SOS Response. *Infect. Immun.* **2015**, *83* (5), 1830−1844.
(53) Ude, J.; Tripathi, V.; Buyck, J. M.; Söderholm, S.; Cunrath, O.; Fanous, J.; Claudi, B.; Egli, A.; Schleberger, C.; Hiller, S.; Bumann, D. Outer Membrane Permeability: Antimicrobials and Diverse Nutrients Bypass Porins in Pseudomonas Aeruginosa. *Proc. Natl. Acad. Sci.* **2021**, *118*, 2107644118.
(54) Naskar, A.; Lee, S.; Lee, Y.; Kim, S.; Kim, K. S. A New Nano-Platform of Erythromycin Combined with Ag Nano-Particle ZnO Nano-Structure against Methicillin-Resistant Staphylococcus Aureus. *Pharmaceutics* **2020**, *12* (9), 841−914.
(55) Naskar, A.; Lee, S.; Kim, K. S. Antibacterial Potential of Ni-Doped Zinc Oxide Nanostructure: Comparatively More Effective against Gram-Negative Bacteria Including Multi-Drug Resistant Strains. *RSC Adv.* **2020**, *10* (3), 1232−1242.
(56) Vaishampayan, A.; Grohmann, E. Antimicrobials Functioning through Ros-mediated Mechanisms: Current Insights. *Microorganisms* **2021**, *10*, 61.
(57) Haktaniyan, M.; Bradley, M. Polymers Showing Intrinsic Antimicrobial Activity. *Chem. Soc. Rev.* **2022**, *51*, 8584−8611.
(58) Lee, Y.; Thompson, D. H. Stimuli-Responsive Liposomes for Drug Delivery. Wiley Interdisciplinary Reviews: Nanomedicine and Nanobiotechnology. *Wiley Interdiscip. Rev.: Nanomed. Nanobiotechnology* **2017**, *9*, 1450.
(59) Hsu, C. F.; Peng, H.; Basle, C.; Travas-Sejdic, J.; Kilmartin, P. A. ABTS●+ Scavenging Activity of Polypyrrole, Polyaniline and Poly(3,4-Ethylenedioxythiophene). *Polym. Int.* **2011**, *60* (1), 69−77.
(60) Nand, A. V.; Ray, S.; Easteal, A. J.; Waterhouse, G. I. N.; Gizdavic-Nikolaidis, M.; Cooney, R. P.; Travas-Sejdic, J.; Kilmartin, P. A. Factors Affecting the Radical Scavenging Activity of Polyaniline. *Synth. Met.* **2011**, *161* (13−14), 1232−1237.

https://doi.org/10.1021/acsomega.3c09871
ACS Omega 2024, 9, 23303−23315